Hindawi
Journal of Nanomaterials
Volume 2017, Article ID 9057250, 6 pages
https://doi.org/10.1155/2017/9057250

Research Article

Hydrogen Gas Sensing Using Palladium-Graphene Nanocomposite Material Based on Surface Acoustic Wave

Nguyen Hai Ha,[1] Nguyen Hoang Nam,[1] Dang Duc Dung,[2] Nguyen Huy Phuong,[1] Phan Duy Thach,[1] and Hoang Si Hong[1]

[1] *School of Electrical Engineering, Hanoi University of Science and Technology (HUST), No. 1 Dai Co Viet Road, Hanoi, Vietnam*
[2] *Department of General Physics, School of Engineering Physics, Hanoi University of Science and Technology (HUST), No. 1 Dai Co Viet Road, Hanoi, Vietnam*

Correspondence should be addressed to Hoang Si Hong; hong.hoangsy@hust.edu.vn

Received 11 March 2017; Accepted 4 May 2017; Published 25 May 2017

Academic Editor: Birol Ozturk

We report the fabrication and characterization of surface acoustic wave (SAW) hydrogen sensors using palladium-graphene (Pd-Gr) nanocomposite as sensing material. The Pd-Gr nanocomposite as sensing layer was deposited onto SAW delay line sensor-based interdigitated electrodes (IDTs)/aluminum nitride (AlN)/silicon (Si) structure. The Pd-Gr nanocomposite was synthesized by a chemical route and deposited onto SAW sensors by air-brush spraying. The SAW H_2 sensor using Pd-Gr nanocomposite as a sensing layer shows a frequency shift of 25 kHz in 0.5% H_2 concentration at room temperature with good repeatability and stability. Moreover, the sensor showed good linearity and fast response/recovery within ten seconds with various H_2 concentrations from 0.25 to 1%. The specific interaction between graphene and SAW transfer inside AlN/Si structures yields a high sensitivity and fast response/recovery of SAW H_2 sensor based on Pd-Gr/AlN/Si structure.

1. Introduction

In order to meet the demands of future hydrogen economy, there are various types of hydrogen (H_2) sensors, which use different mechanisms (e.g., resistance based, optical based, catalyst based, electrochemical based, thin and thick film based, chemochromic based, Schottky based, MEMS-based, and surface acoustic wave (SAW) based) to detect H_2 gas [1]. A method for precisely detecting hydrogen with high sensitivity and selectivity and fast response is required for the development of hydrogen energy economy as well as environmental protection and human safety. Among these sensors, the SAW sensor has advantages that allow for remote wireless operation and a high potential in passive sensors [1, 2].

Among various sensing materials and noble metal catalysts for H_2 sensors, palladium (Pd) nanoparticles (NPs) are well known and popular for H_2 sensing detectors due to their high sensitivity, good selectivity, and ability to operate at room temperature. In addition, Pd NPs expand their volume to a few percent during H_2 absorption/desorption, which can easily cause nonstructural stability in sensors [3]. In order to mitigate these problems, recently, graphene has been shown to have excellent properties as a potential material to support Pd NP catalyst or form Pd-graphene (Pd-Gr) nanocomposites [3] and has shown attractive results for H_2 sensing in terms of high sensitivity and stability.

However, applying these Pd-Gr composites for H_2 detection is still limited to a resistivity type [3, 4]. The SAW gas sensor has been widely investigated due to several attractive advantages including high sensitivity, small size, reliability, and wireless ability [5, 6]. In addition, graphene is promising to develop SAW sensors because of its planar 2D crystal structure and specific sensitivity with electric field and acoustic wave [7–12]. Most of the previously used SAW devices are based on traditional bulk substrates such as quartz, $LiNbO_3$, and $LiTaO_3$ due to their high electromechanical coupling coefficient, but their poor temperature stability leads to reliability problems [7–12]. In fact, the temperature stability of the SAW sensor is a significant problem in designing a sensor that avoids the interference of ambient temperature with actual sensing characteristics [13]. The AlN films were proven to benefit SAW applications because of the high

acoustic velocity, superior temperature, chemical stability, and compatibility with the MEMS process [13]. In addition, compared to the temperature coefficient of frequency (TCF) of traditional bulk substrates such as $LiNbO_3$ and $LiTaO_3$ (upper −40 ppm/°C), that of AlN/Si (−30 ppm/°C) is significantly smaller, which can reduce the influence of the outside temperature [13].

Recently, graphene was reported as superior for sensing materials with advantages of high sensitivity and fast response [14]. In addition to these advantages, defective/functionalized graphene and graphene-based nanocomposite were applied in sensing field with many kinds of sensing mechanisms [15–18]. Nevertheless, graphene-based SAW sensors have been limited by few reports [7–12], especially the SAW sensor using piezoelectric thin films as AlN and graphene, in which the interaction between graphene and AlN interface has never been reported yet. Hence, in this work, we tried developing a SAW H_2 sensor based on Pd-Gr composite using AlN thin films; the properties of the SAW H_2 sensor were investigated and discussed in detail in this paper.

2. Experimental Section

High-quality polycrystalline piezoelectric (002)-oriented AlN thin films, 2 μm thick (h), were deposited on (100)-Si wafers by a pulsed reactive magnetron sputtering system [13]. The two-port SAW delay lines based on IDT/AlN/Si were constructed using conventional photolithography and lift-off process. Gold (Au) with thickness of 100 nm prepared by RF sputtering was used for IDT. We used IDTs of 50 finger pairs with an electrode period (d) of 10 μm. The aperture was $100\lambda = 4000\,\mu$m. The IDT-IDT gap was 5 mm. The wavelength ($\lambda = 4d$) was 40 μm.

Graphene oxide (GO) was prepared from extra pure graphite powder (Merck, 99.99%) according to Hummers method. Pd-Gr nanocomposites were synthesized by a simple, one-step process using 25 mL of a GO aqueous solution (with fixed concentration of 1 mg/mL) and 25 mL of DI water containing 0.25 mg/mL concentrations of palladium chloride ($PdCl_2$, Aldrich, 99%) [3]. First, 25 mL of the GO solution was mixed with 25 ml $PdCl_2$, followed by adding 500 μL hydrazine monohydrate ($N_2H_4{\cdot}H_2O$, Aldrich, 65 wt.%) as a reduction agent with rigorous stirring. The resulting 50 mL stable suspension, which was black, was used to fabricate SAW sensors. In brief, Pd-Gr composites were deposited on an AlN/Si substrate on the selected area via a mask by airbrush spraying from 2 mL above the suspension. The AlN/Si substrate was heated on a hot plate at 200°C during spraying.

Hydrogen gas sensing characteristics of the SAW sensor were tested for various hydrogen concentrations at room temperature (25°C) and relative humidity (RH) level of 30%. The sensor was mounted inside an enclosed environmental chamber. The characteristics of the two-port SAW sensor were measured with an Agilent 8802A Network Analyzer. The frequency shift of the SAW sensor was recorded by a frequency counter (Agilent 53181A) connected to a laptop via a General-Purpose Interface Bus (GPIB) card. A computerized mass flow controller system was used to vary the concentration of H_2 in synthetic air (0.25%, 0.5%, 0.75%, and 1%). The gas mixture was delivered to the chamber at a constant flow rate of 50 sccm (standard cubic centimeters per minute). The gas exposure time was fixed for each pulse of H_2 gas and the cell was purged with synthetic air between each pulse to allow the surface of the sensor to recover to atmospheric conditions. The crystalline characteristics of the Pd-Gr composite on the AlN/Si structure were investigated using X-ray diffraction (XRD) with CuKα radiation (1.54178 Å). The surfaces of the thin films were characterized using a JEOL model 7600F field emission scanning electron microscope (FE-SEM). The Raman spectra were collected by a HORIBA Raman.

3. Result and Discussion

Figure 1(a) shows the SEM images of pure AlN/Si substrate. The surface of AlN thin film, which was prepared by pulsed reactive magnetron sputtering system, was smooth and consisted of grain size of 50 nm. Figure 1(b) shows the SEM images of Pd-Gr nanocomposite depositing on the AlN/Si substrate. The Pd NPs were well isolated and decorated on the graphene flakes with a high density of Pd NPs. Figure 1(c) shows the TEM image of as-synthesized Pd-Gr nanocomposites. The Pd NPs with size of around 10 nm are well dispersed and wrapped into graphene flakes as shown in Figures 1(b) and 1(c). The Pd-Gr formed like core-shell structures and Pd lattice constant was 0.23 nm. Figure 1(d) shows selected area electron diffraction (SAED) of Pd-Gr composites.

Figure 2 shows the XRD patterns of the Pd-Gr/AlN/Si structure. The peaks of the graphene in the XRD spectra did not clearly appear due to high intensity ratio of AlN peaks/Pd-Gr composites peaks. Other peaks appearing at $2\theta = 36.08^\circ$ and 76.47° indicated (002) and (004) planes of the AlN film (JCPDS 00-065-0831). Among the peaks related to the hexagonal structure of the AlN film, the strongest peak appeared at $2\theta = 36.08^\circ$, which proves that the poly-AlN film had the (002) dominant oriented plane [13]. The full width at half maximum (FWHM) of the rocking curve at the (002) peak of the AlN films was 0.19°. The small FWHM values of the preferred (002) peak of the AlN thin film indicated the high quality of the films, which is very important for estimation of piezoelectric properties of AlN [13]. The peak at $2\theta = 40.44^\circ$ (JCPDS 01-087-0645) corresponding to the Pd(111) plane confirmed the presence of Pd in the structure.

Figure 3 shows Raman spectra of the pure AlN/Si and Pd-Gr/AlN/Si structure. The peak at 521 cm^{-1} indicates Si substrate. The peak at 653 cm^{-1} is correlated to the first-order vibrational mode of E_2 (high) of AlN thin film [19]. The Raman spectrum of Pd-Gr composite consists of two major sharp peaks: G and D peaks. The features of those peaks are the indicators of the quality of graphene such as doping and strain. The G peak at 1590 cm^{-1} corresponds to the first-order scattering of the E_{2g} mode. A prominent D peak at 1330 cm^{-1} is related to defects present [3].

Figure 4(a) shows schematic of the fabricated sensor with coating Pd-Gr composites. The SAW sensor of pure AlN/Si without coating Pd-Gr composite has resonant frequency of 128.78 MHz and attenuation of −23.73 dB as shown in Figure 4(b). Figure 4(c) shows the frequency responses of the two-port SAW delay with coating Pd-Gr nanocomposite.

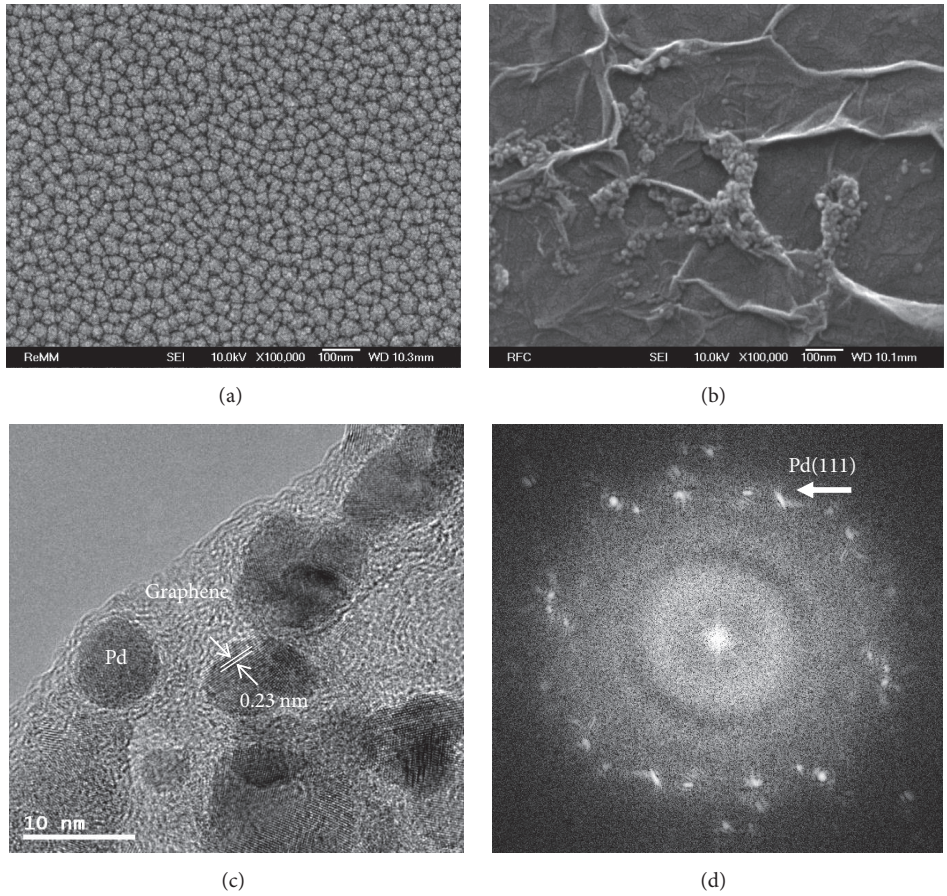

Figure 1: SEM images of (a) pure AlN/Si, (b) Pd-Gr composite on AlN/Si, (c) TEM image of Pd-Gr composite, and (d) SAED analysis of Pd-Gr composite.

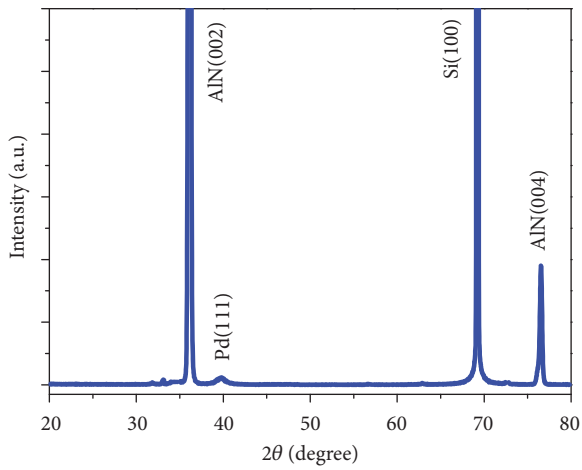

Figure 2: XRD spectra of Pd-Gr/AlN/Si structure.

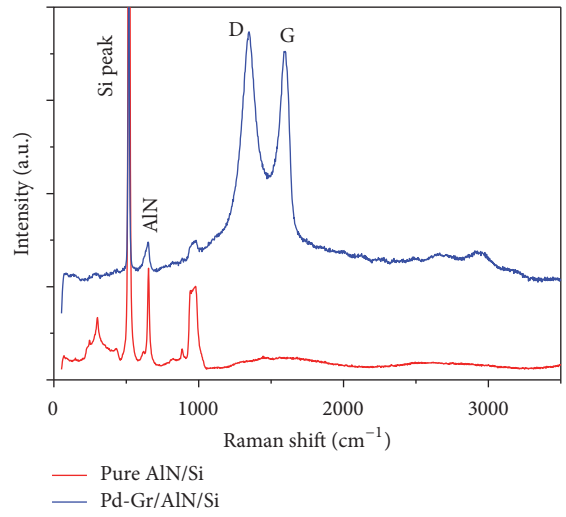

Figure 3: Raman spectra of pure AlN/Si and Pd-Gr/AlN/Si structure.

The SAW sensor of Pd-Gr/AlN/Si has resonant frequency of 126.54 MHz and attenuation of −26.76 dB. The SAW velocities were evaluated by measuring the center frequency (f_0) and λ of the SAW delay line and applying the equation $f_0 = V_{SAW}/\lambda$. After the Pd-Gr composite was coated onto the AlN/Si structure, the SAW velocity of the Pd-Gr/AlN/Si structure was reduced to approximately 5062 m/s while that of the pure AlN/Si structure was 5151 m/s. Additionally, the

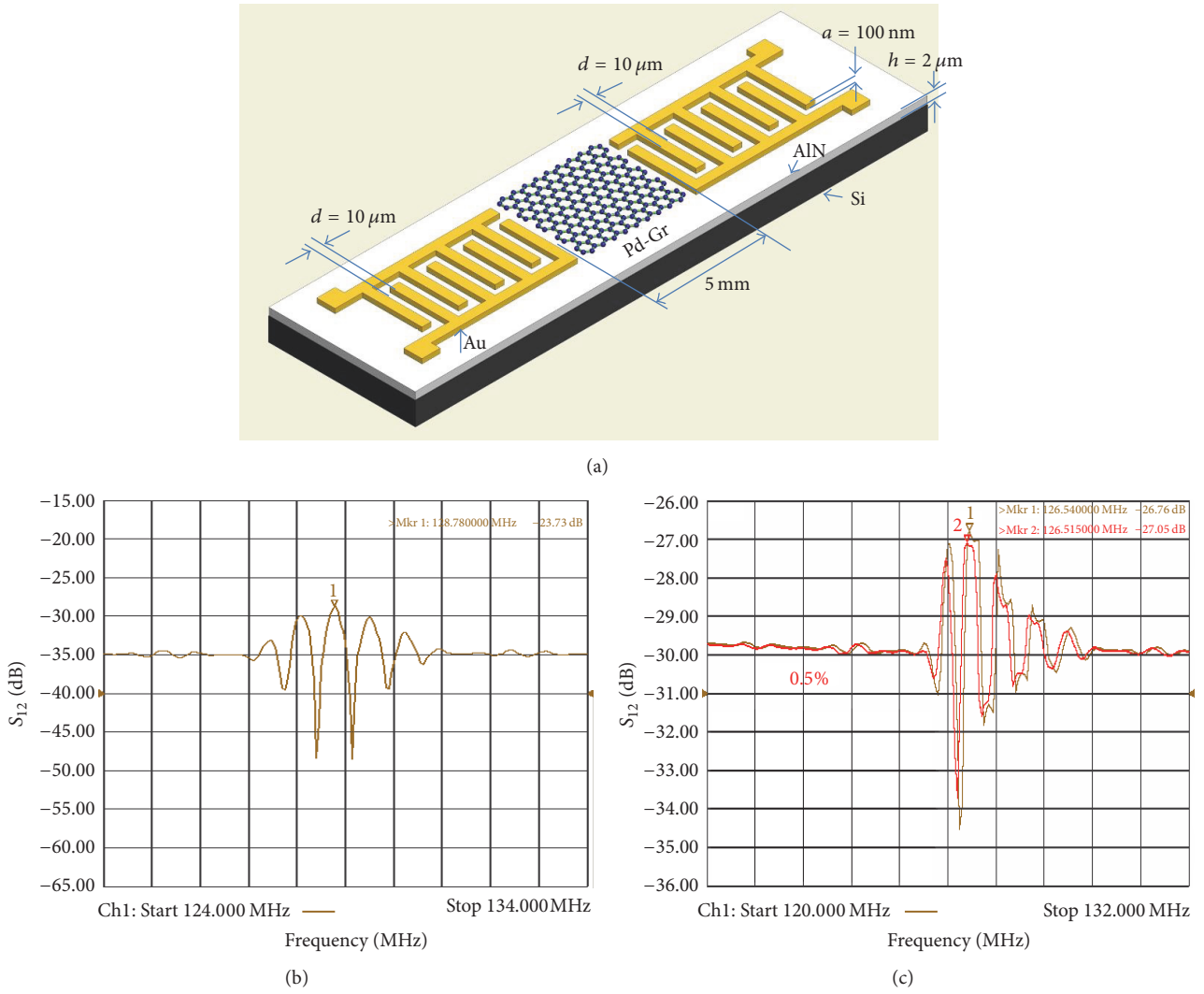

FIGURE 4: (a) Schematic of the fabricated SAW H_2 sensor with coating Pd-Gr composite, frequency response of a SAW H_2 sensor of (b) pure AlN/Si structure and (c) Pd-Gr/AlN/Si structure at 0.5% hydrogen concentration at room temperature (30% RH).

attenuation of the structures was increased by 3.03 dB. These changes may originate from the change in the mass loading and high conductivity in the coated Pd-Gr nanocomposite. In fact, the Pd-Gr nanocomposite coating degrades resonant phenomenon in a SAW delay line [5, 6]. The results of the research can indicate a possible effect of the high conductivity of the Pd-Gr that degrades the acoustic transmission, as it is shown in Figures 4(b) and 4(c) (around 3 dB between acoustic and electromagnetic signals), which has negative effects, such as a strong noise in the resonant frequency [5].

Figure 4(c) shows the frequency responses of the two-port SAW delay line coated with Pd-Gr nanocomposite with 0.5% H_2 at room temperature (25°C). The frequency down shifts of 25 kHz at 0.5% hydrogen concentration were observed in Figure 4(c). The attenuation of the structures was increased by 0.29 dB. The hydrogen atoms are decomposed to hydrogen ions (protons) and free electrons by the Pd catalytic reaction even at room temperature. These free electrons were transferred to the p-type graphene, reduced conductivity in the Pd-Gr composite [3], interacted with the electric field accompanying the propagating SAW [12], and modified the SAW properties, resulting in increased attenuation and a shift down resonant frequency in the SAW delay line [2, 5–9]. In Figure 4(c), the mass loading effect is insignificant in the frequency shift due to H_2 interaction; therefore, a SAW sensor, with acoustic transmission degraded, is used to detect conductivity changes due to the interaction of Pd-Gr composite with H_2. In our previous work [3], a resistive sensor based on Pd-Gr composite was used to measure conductivity changes of Pd-Gr, showing better results than the SAW sensor. Therefore, the resistive sensor detected the minimum H_2 concentration of 0.2 ppm [3], in contrast with the present work in which the lowest concentration detected by means of SAW sensor was 0.25% (2500 ppm).

Figure 5(a) shows transient response of H_2 sensor with various H_2 concentrations from 0.25 to 1%. The sensor showed the different response level to different H_2 concentrations with linearity and fast response/recovery. The response

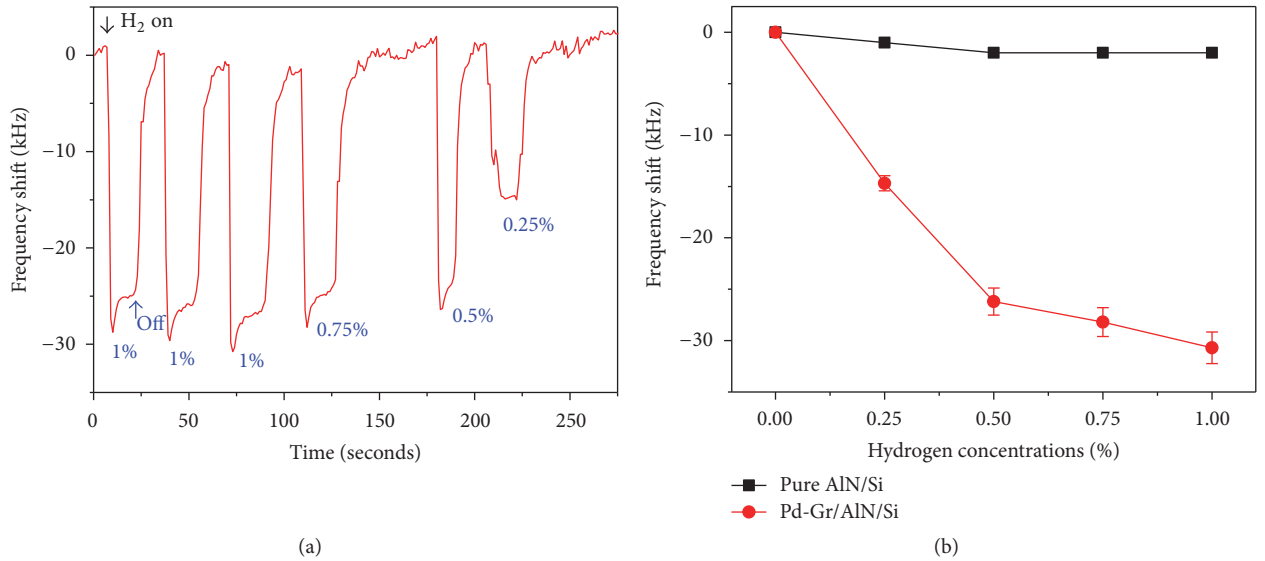

FIGURE 5: (a) Transient response of H_2 sensor with various H_2 concentrations and (b) the linearity of the sensor at room temperature.

time is defined as the time required for the H_2 sensor to reach 90% of the frequency shift (Δf) when the sensor is exposed to a given concentration of hydrogen. The recovery time is defined as the time needed to recover 90% of the initial baseline after hydrogen turn-off. The response/recovery time of SAW sensor estimated from responses in Figure 5(a) is 1/9 seconds with 1% H_2 at room temperature. Figure 5(b) shows sensor response at various H_2 concentrations; the resonant frequency of the structure without Pd-Gr composite (control device) did not demonstrate any change because of the stability of the AlN films in the presence of hydrogen. The small shift of SAW sensor without Pd-Gr composite (1-2 kHz) was caused by the moisture effect created by different levels of H_2 gas concentration in the chamber. However, the negligible shift was in the error range of testing measurement. In contrast, the resonant frequency of SAW sensors with the coated Pd-Gr composite was clearly shifted. These changes may originate from the change in the mass loading and conductivity in the coated Pd-Gr composite as H_2 sensing layer. In comparison with previous works as pure graphene-based SAW H_2 sensor on $LiTaO_3$ substrate [8] (frequency shift of 6 kHz, response/recovery time of 75/500 seconds with 1% H_2) or Pt/ZnO-based SAW H_2 sensor on AlN/Si substrate [2] (frequency shift of 55 kHz, response/recovery time of few minutes with 1% H_2), our SAW H_2 sensor of Pd-Gr/AlN/Si structure in this work (frequency shift of 30 kHz, response/recovery time of 1/9 seconds with 1% H_2) had advantages of higher sensitivity and faster response. Thanks to the advantages of graphene as high electron mobility and specific graphene/AlN interface, the SAW H_2 sensor in this work has very fast response and recovery time [12].

4. Conclusion

We demonstrated the SAW H_2 sensor using Pd-Gr composite based on AlN/Si structure. The SAW H_2 sensor has higher sensitivity and fast response because of the accompanying effect of the graphene/AlN interface. In addition, graphene has a planar 2D crystal structure and has specific sensitivity with electric field accompanying the propagating SAW inside the AlN thin film. The SAW hydrogen sensor shifted to a maximum at 30 kHz in a 1% hydrogen concentration and showed a linear response in the range of 0.25 to 1% hydrogen at room temperature. The SAW sensor has fast response/recovery time of 1/9 seconds with 1% H_2 at room temperature. In addition, the sensor has good repeatability in both H_2 cycle testing and different response to various H_2 concentrations.

Conflicts of Interest

The authors declare that there are no conflicts of interest regarding the publication of this paper.

Acknowledgments

This research is funded by Vietnam National Foundation for Science and Technology Development (NAFOSTED) under Grant no. 103.02-2014.47.

References

[1] T. Hübert, L. Boon-Brett, V. Palmisano, and M. A. Bader, "Developments in gas sensor technology for hydrogen safety," *International Journal of Hydrogen Energy*, vol. 39, no. 35, pp. 20474–20483, 2014.

[2] D.-T. Phan and G.-S. Chung, "Surface acoustic wave hydrogen sensors based on ZnO nanoparticles incorporated with a Pt catalyst," *Sensors and Actuators, B: Chemical*, vol. 161, no. 1, pp. 341–348, 2012.

[3] D.-T. Phan and G.-S. Chung, "Characteristics of resistivity-type hydrogen sensing based on palladium-graphene nanocomposites," *International Journal of Hydrogen Energy*, vol. 39, no. 1, pp. 620–629, 2014.

[4] U. Lange, T. Hirsch, V. M. Mirsky, and O. S. Wolfbeis, "Hydrogen sensor based on a graphene-palladium nanocomposite," *Electrochimica Acta*, vol. 56, no. 10, pp. 3707–3712, 2011.

[5] H.-S. Hong and G.-S. Chung, "Controllable growth of oriented ZnO nanorods using Ga-doped seed layers and surface acoustic wave humidity sensor," *Sensors and Actuators, B: Chemical*, vol. 195, pp. 446–451, 2014.

[6] G. Zhang, "Nanostructure-enhanced surface acoustic waves biosensor and its computational modeling," *Journal of Sensors*, vol. 2009, Article ID 215085, 11 pages, 2009.

[7] R. Arsat, M. Breedon, M. Shafiei et al., "Graphene-like nanosheets for surface acoustic wave gas sensor applications," *Chemical Physics Letters*, vol. 467, no. 4–6, pp. 344–347, 2009.

[8] R. Arsat, M. Breedon, M. Shafiei et al., "Graphene-like nanosheets/36◦ liTaO3 surface acoustic Wave hydrogen gas sensor," in *Proceedings of the IEEE Sensors, SENSORS 2008*, pp. 188–191, October 2009.

[9] S. Thomas, M. Cole, A. De Luca et al., "Graphene-coated rayleigh SAW resonators for NO_2 detection," *Procedia Engineering*, vol. 87, pp. 999–1002, 2014.

[10] S. M. Balashov, O. V. Balachova, A. V. U. Braga, A. P. Filho, and S. Moshkalev, "Influence of the deposition parameters of graphene oxide nanofilms on the kinetic characteristics of the SAW humidity sensor," *Sensors and Actuators, B: Chemical*, vol. 217, Article ID 17690, pp. 88–91, 2015.

[11] I. Sayago, D. Matatagui, M. J. Fernández et al., "Graphene oxide as sensitive layer in Love-wave surface acoustic wave sensors for the detection of chemical warfare agent simulants," *Talanta*, vol. 148, pp. 393–400, 2016.

[12] V. Miseikis, J. E. Cunningham, K. Saeed, R. O'Rorke, and A. G. Davies, "Acoustically induced current flow in graphene," *Applied Physics Letters*, vol. 100, no. 13, Article ID 133105, 2012.

[13] S.-H. Hoang and G.-S. Chung, "Surface acoustic wave characteristics of AlN thin films grown on a polycrystalline 3C-SiC buffer layer," *Microelectronic Engineering*, vol. 86, no. 11, pp. 2149–2152, 2009.

[14] S. S. Varghese, S. Lonkar, K. K. Singh, S. Swaminathan, and A. Abdala, "Recent advances in graphene based gas sensors," *Sensors and Actuators B: Chemical*, vol. 218, pp. 160–183, 2015.

[15] Y. Jiang, S. Yang, S. Li, W. Liu, and Y. Zhao, "Highly sensitive co gas sensor from defective graphene: role of van der waals interactions," *Journal of Nanomaterials*, vol. 2015, Article ID 504103, 7 pages, 2015.

[16] S. Yoo, X. Li, Y. Wu, W. Liu, X. Wang, and W. Yi, "Ammonia gas detection by tannic acid functionalized and reduced graphene oxide at room temperature," *Journal of Nanomaterials*, vol. 2014, Article ID 497384, 6 pages, 2014.

[17] S.-H. Yu and G. C. Zhao, "Preparation of platinum nanoparticles-graphene modified electrode and selective determination of rutin," *International Journal of Electrochemistry*, vol. 2012, Article ID 431253, 6 pages, 2012.

[18] C.-L. Sun, J.-S. Su, S.-Y. Lai, and Y.-J. Lu, "Size effects of Pt nanoparticle/graphene composite materials on the electrochemical sensing of hydrogen peroxide," *Journal of Nanomaterials*, vol. 2015, Article ID 861061, 7 pages, 2015.

[19] W. Lei, J. Zhang, D. Liu, P. Zhu, Q. Cui, and G. Zou, "Three-dimensional AlN microroses and their enhanced photoluminescence properties," *Chemical Communications*, no. 41, pp. 5221–5223, 2008.